

NUMERICAL CALCULATION OF THE FLOW OF A CONDUCTING FLUID  
BETWEEN ROUGH SURFACES IN A TRANSVERSE MAGNETIC FIELD

G. G. Branover, G. A. Vitolin'sh, R. K. Dukure, R. P. Zolberga, Kh. E. Kalis, and A. B. Tsinober

Magnitnaya Gidrodinamika, Vol. 3, No. 3, pp. 105-111, 1967

UDC 538.4

The Navier-Stokes equations for flow between parallel rough surfaces in the presence of a transverse magnetic field are solved. The results obtained by numerical calculation are compared qualitatively with the experimental data. It is established that roughness has an important effect on the resistance coefficient for laminar flow in the presence of a magnetic field.

In the absence of a magnetic field the roughness of the channel walls usually has no effect on the resistance coefficient in laminar flow. This is also known

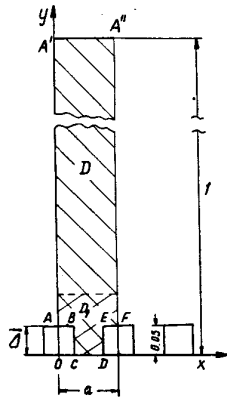


Fig. 1. Diagram of flow region.

from Nikuradse's experiment [1]. As the data presented in that paper show, in the presence of a transverse field wall roughness does have an effect on resistance, which increases with the intensity  $H$ . It should be noted that the density of the surface irregularities is also important. When the irregularities are very thinly distributed, their effect on resistance may be almost imperceptible, even in the presence of a transverse magnetic field [2].

In order to establish the principles of flow between rough surfaces in a transverse magnetic field we undertook a numerical solution of the differential equations of motion. There have already been attempts to calculate numerically the flow in an isolated slot when the boundary conditions are given directly at the edge [3, 4] or at a distance from the slot commensurable with its dimensions [5]. We are interested in the case when the height of the slot is much less than the dimension of the channel and when the slots recur periodically at definite linear intervals.

The following notation is employed:  $R$  is a characteristic dimension equal to half the distance between the rough surfaces from the bottom of a slot in one surface to the bottom of a slot in the other surface;  $\Delta$  the height of a slot divided by  $R$ ;  $k$  the height of a

slot;  $u_m$  the mean velocity calculated along the dimension  $R$ ;  $B_0$  the induction of the external magnetic field;  $Re$  the dynamic Reynolds number;  $Re_m$  the magnetic Reynolds number;  $N$  the Stewart number;  $M$  the Hartmann number.

**Formulation of the problem and method of solution.** We have examined the plane-parallel flow of an incompressible viscous conducting fluid in a transverse magnetic field between parallel surfaces with periodically recurring square steps of relative height 0.05 (Fig. 1). The distance between steps was also 0.05. The problem was solved in the inductionless approximation, i. e., when  $Re_m \ll 1$ . In this case the equations of plane parallel motion are written in dimensionless form as follows\*:

$$\begin{aligned} u \frac{\partial u}{\partial x} + v \frac{\partial u}{\partial y} &= -\frac{\partial p}{\partial x} + \frac{1}{Re} \Delta u + N(E_z - u); \\ u \frac{\partial v}{\partial x} + v \frac{\partial v}{\partial y} &= -\frac{\partial p}{\partial y} + \frac{1}{Re} \Delta v; \quad \frac{\partial u}{\partial x} + \frac{\partial v}{\partial y} = 0 \end{aligned} \quad (1)$$

with the boundary conditions

$$u|_s = v|_s = 0 \text{ on the solid boundary } s;$$

$$\frac{\partial u}{\partial y} \Big|_{y=1} = v|_{y=1} = 0 \text{ on the axis of symmetry } A'A'' \quad (2)$$

and the constant flow rate condition  $\int_0^1 u dy = 1$ .

In addition, we specified the conditions of periodicity on the lines  $x = 0$  and  $x = a$ ,

$$\begin{aligned} u|_{x=0} &= u|_{x=a}; \quad v|_{x=0} = v|_{x=a}; \\ \frac{\partial u}{\partial x} \Big|_{x=0} &= \frac{\partial u}{\partial x} \Big|_{x=a}; \quad \frac{\partial v}{\partial x} \Big|_{x=0} = \frac{\partial v}{\partial x} \Big|_{x=a}. \end{aligned} \quad (3)$$

For plane-parallel flow the electric field  $E_z$  is constant. It can be found from the condition of zero total current in the region  $D$ . This gives

$$E_z = (1 - \bar{\Delta}/2)^{-1}.$$

By introducing the stream function  $\psi$  ( $u = \partial\psi/\partial y$ ,  $v = -\partial\psi/\partial x$ ) we reduce the system of Navier-Stokes equations to the equation

\*As the characteristic quantities we took  $\rho u_m^2$ , and  $u_m B_0$ .

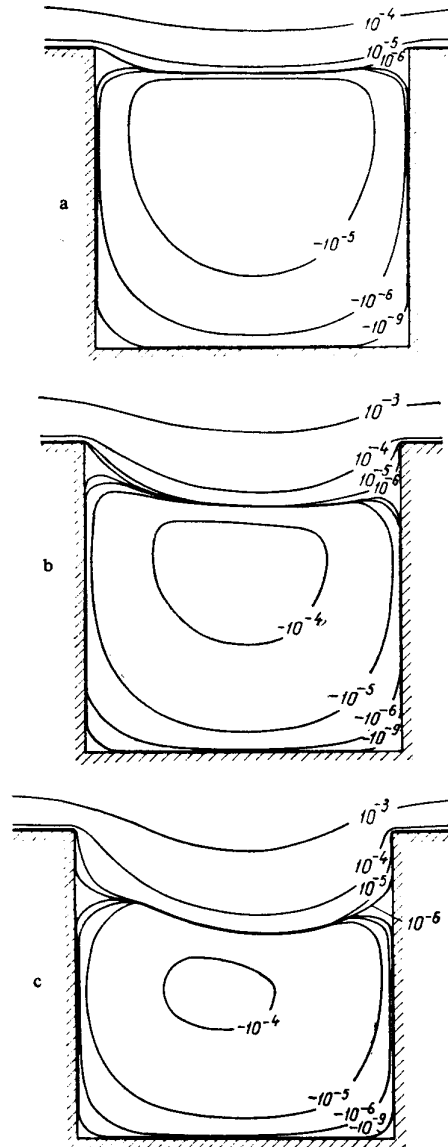


Fig. 2. Streamline patterns at  $Re = 200$ . a)  $N = 0$ ; b)  $N = 3$ ; c)  $N = 9$ .

$$L\psi = \frac{1}{\text{Re}} \Delta \Delta \psi + \frac{\partial \psi}{\partial x} \frac{\partial \Delta \psi}{\partial y} - \frac{\partial \psi}{\partial y} \frac{\partial \Delta \psi}{\partial x} - N \frac{\partial^2 \psi}{\partial y^2} = 0. \quad (4)$$

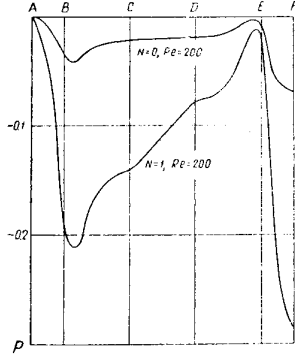


Fig. 3. Pressure distribution.

In this case boundary conditions (2) are written in the following form:

$$\psi|_s = 0, \quad \frac{\partial \psi}{\partial n} \Big|_s = 0 \text{ on the solid boundary } s, \quad (5)$$

$$\psi|_{y=1} = 1, \quad \frac{\partial^2 \psi}{\partial y^2} \Big|_{y=1} = 0 \text{ on the axis of symmetry } A'A''$$

and the conditions of periodicity (3)

$$\begin{aligned} \psi|_{x=0} = \psi|_{x=a}; \quad \frac{\partial \psi}{\partial x} \Big|_{x=0} = \frac{\partial \psi}{\partial x} \Big|_{x=a}; \\ \frac{\partial^2 \psi}{\partial x^2} \Big|_{x=0} = \frac{\partial^2 \psi}{\partial x^2} \Big|_{x=a}. \end{aligned} \quad (6)$$

As the initial conditions we took the distribution of the stream function corresponding to Poiseuille and Hartmann flow at  $N = 0$  and  $N \neq 0$ , respectively, for the channel half-width  $1 - \bar{\Delta}$

$$\psi = \begin{cases} \frac{M(y - \bar{\Delta}) \text{ch } M(1 - \bar{\Delta}) + \text{sh } M(1 - y) - \text{sh } M(1 - \bar{\Delta})}{M(1 - \bar{\Delta}) \text{ch } M(1 - \bar{\Delta}) - \text{sh } M(1 - \bar{\Delta})}; \\ \frac{3(y - \bar{\Delta})(1 - \bar{\Delta})^2 + (1 - y)^3 - (1 - \bar{\Delta})^3}{2(1 - \bar{\Delta})^3}. \end{cases} \quad (7)$$

The solution of Eq. (4) with boundary conditions (5) and periodicity conditions (6) was found as the limit of the solution of the corresponding nonstationary problem as  $t \rightarrow \infty$ . In this case Eq. (4) takes the form

$$L\psi = \frac{\partial \Delta \psi}{\partial t}. \quad (8)$$

Since the height of the step is only 5% of the width between surfaces, to establish the nature of the flow between steps it is necessary to use a very fine grid. This, in turn, leads to a very large expenditure of machine time. Therefore the calculations were made not over the entire region  $D$ , but only in the region  $D_1$  (see Fig. 1). Elsewhere in  $D - D_1$  it was assumed that the flow coincides with Hartmann flow. The height of the region  $D_1$  was about twice the step height.

We introduced the spatial grid

$$x = ih, \text{ where } i = 0, 1, 2, \dots, n,$$

$$y = jl, \text{ where } j = 0, 1, 2, \dots, m,$$

$h, l$  are the steps in the direction of the  $x$  and  $y$  axes, respectively.

Specifically, we took the following parameters:  $n = 8, 12, 16$ ;  $m = 10, 14, 20$ ;  $h, l = 0.0125; 0.0083; 0.00625$ . The values of the  $\text{Re}$  and  $N$  numbers were  $\text{Re} = 50, 200, 600$ ;  $N = 0, 1, 3, 9$ .

In this case the entire external and internal immediate-access memory of the machine was fully utilized.

In order to verify the correctness of calculations limited to the region  $D_1$ , we made calculations by another method over the entire region  $D$ .

Equation (4) was reduced to a system of two equations by introducing the curl function

$$\begin{aligned} \frac{1}{\text{Re}} \Delta \xi + \frac{\partial \psi}{\partial x} \frac{\partial \xi}{\partial y} - \frac{\partial \psi}{\partial y} \frac{\partial \xi}{\partial x} + N \frac{\partial^2 \psi}{\partial y^2} = 0; \\ \xi = -\Delta \psi. \end{aligned} \quad (9)$$

To the boundary conditions (5) we added the conditions for  $\xi$ :

$$\xi|_{y=1} = 0. \quad (10)$$

At the solid surface we assigned conditions that are obtained by expanding the function  $\psi$  in a Taylor series. In this case we discarded terms of order greater than  $h^2$  and used the second equation of system (9) at the boundary.

From the periodicity conditions it follows that

$$\xi|_{x=0} = \xi|_{x=a}. \quad (11)$$

To obtain the solution we used the grid  $x = ih$  ( $i = 0, 1, 2, \dots, n$ ),  $h = 0.00625$ ,  $n = 16$ ,  $l = 0.00625$  to  $y = 0.075$ ;  $l = 0.0125$  to  $y = 0.125$ ;  $l = 0.025$  to  $y = 0.2$ ;  $l = 0.05$  to  $y = 0.3$ ;  $l = 0.1$  to  $y = 1$ , where  $h, l$  are the steps in the direction of the  $x$  and  $y$  axes, respectively. The values of the  $\text{Re}$  and  $N$  numbers were  $\text{Re} = 200, N = 0, 1, 3$ ;  $\text{Re} = 600, N = 0, 1$ .

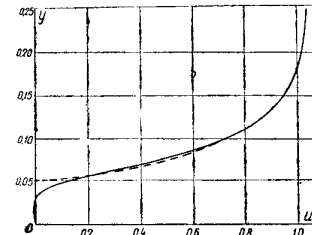


Fig. 4. Velocity profiles.

In the course of the calculation, (8) was replaced by a finite-difference equation of the form

$$\begin{aligned} \frac{\Delta \psi^{k+1} - \Delta \psi^k}{\tau} = \frac{1}{\text{Re}} \Delta^2 \psi^{k+1} + \\ + (1 - \alpha) \left[ \frac{\partial \psi^k}{\partial x} \frac{\partial \Delta \psi^{k+1}}{\partial y} - \frac{\partial \psi^k}{\partial y} \frac{\partial \Delta \psi^{k+1}}{\partial x} \right] + \end{aligned}$$

$$+ \alpha \left[ \frac{\partial \psi^{k+1}}{\partial x} \frac{\partial \Delta \psi^k}{\partial y} - \frac{\partial \psi^{k+1}}{\partial y} \frac{\partial \Delta \psi^k}{\partial x} \right] - N \frac{\partial^2 \psi^{k+1}}{\partial y^2}, \quad (12)$$

where  $0 \leq \alpha \leq 1$ ,  $\psi^k$  is the value of  $\psi$  in the  $k$ -th time interval, or at  $t = k\tau$  ( $\tau$  is the time step,  $k = 1, 2, \dots$ ,  $\dots$ ,  $\tau = 0.5; 0.25$ ).

Correspondingly, system (9) was replaced with the finite-difference equations

$$\begin{aligned} \frac{\xi^{k+1} - \xi^k}{\tau} &= \frac{1}{\text{Re}} \Delta \xi^{k+1} + \frac{\partial \psi^k}{\partial x} \frac{\partial \xi^{k+1}}{\partial y} - \\ &- \frac{\partial \psi^k}{\partial y} \frac{\partial \xi^{k+1}}{\partial x} + N \frac{\partial^2 \psi}{\partial y^2}; \\ \xi^{k+1} &= -\Delta \psi^{k+1}. \end{aligned} \quad (13)$$

The following time steps were taken:  $\tau = 0.01, 0.05$ . The solution did not converge for  $\tau = 0.05$ .

In order to construct the finite-difference equations we took the central differences with order of approximation  $h^2 + l^2$ . Finally, in Eq. (12) the parameter  $\alpha$  was taken equal to zero, since the use of other values of  $\alpha$  did not give any improvement in convergence.

The difference equations in explicit form are too clumsy to write out.

Equations (12), (13) were solved by the method of nets using matrix pivotal condensation formulas [6, 7]. On each time interval the difference equations (13) were solved separately in the slot and in the region outside it and the solutions joined on the line ABEF.

The results obtained by the two methods differ slightly. When the roughness distribution is very thin, e.g.,  $a = 20k$ ,  $AB = EF = 2k$ , the first method of calculation is not suitable in the neighborhood of a step, since in this case the flow immediately above the step differs considerably from Hartmann flow.

RESULTS OF CALCULATION

1. **Streamline pattern.** A standard program was used to find the streamlines from known values of the stream function  $\psi$  at the nodes of the grid. Figure 2 shows the streamline pattern for three values of  $N$  at  $\text{Re} = 200$ . It is clear from the figures that the main stream penetrates further and further into the slot as  $N$  increases, while the size of the eddy is curtailed. Thus, as  $N$  increases, an ever greater part of the height of the step enters into the main stream, i.e., the effective relative roughness increases. This pattern closely resembles that observed in connection with flow past a body in a transverse magnetic field [8], when the flow behind the body approaches closer and closer to the unseparated state as the strength of the magnetic field increases.

2. **Pressure distribution over surface.** The pressure distribution at the wall was found from stationary equations (1) using boundary conditions (2) and (3). On the horizontal lines the pressure was found from the equations

$$p = p_0 + NE_x x + \frac{1}{\text{Re}} \int_{x_0}^x \frac{\partial^3 \psi}{\partial y^3} dx, \quad (14)$$

where  $p_0 = 0$ ;  $x_0 = 0$  on AB;  $p_0 = p(C)$ ;  $x_0 = a/4$  on CD;  $p_0 = p(E)$ ;  $x_0 = 3a/4$  on EF.

On the vertical lines the pressure was found from

$$p = p_0 - \frac{1}{\text{Re}} \int_{y_0}^y \frac{\partial^3 \psi}{\partial x^3} dy, \quad (15)$$

where  $p_0 = p(B)$ ;  $y_0 = a$  on BC;  $p_0 = p(D)$ ;  $y_0 = 0$  on DE.

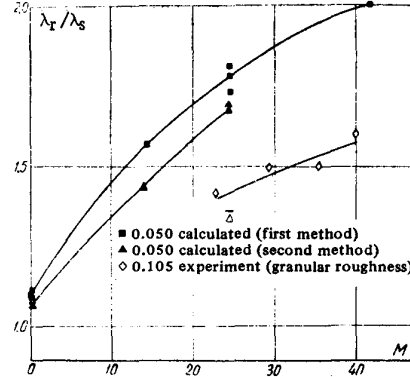


Fig. 5. Relative resistance coefficient as a function of Hartmann number.

The integrals were calculated from the trapezoidal rule. The pressure distribution at the surface is shown in Fig. 3 for  $\text{Re} = 200, N = 0$  and  $N = 1$ . It is clear from the figure that under the influence of a magnetic field the pressure difference between the front and rear walls of the step increases considerably.

3. **Velocity distribution.** The dimensionless velocities were found from the relations

$$u = \frac{\partial \psi}{\partial y}; \quad v = -\frac{\partial \psi}{\partial x}$$

by means of the approximation

$$\begin{aligned} u &= \frac{\psi(x, y+l) - \psi(x, y-l)}{2l}; \\ v &= -\frac{\psi(x+h, y) - \psi(x-h, y)}{2h}. \end{aligned} \quad (16)$$

The dimensionless velocity profiles obtained by the two calculation methods differ by not more than 5%. Figure 4 shows the dimensionless velocity distribution for  $N = 3$ ;  $\text{Re} = 200$  and the almost identical distribution for  $N = 1$ ;  $\text{Re} = 600$ . This correspondence may be attributed to the fact that in both cases the Hartmann number was the same. The solid curve corresponds to the velocity profile on the line  $x = a/2$  (at the center of the slot), the broken line to the velocity profile on the line  $x = a$  (see Fig. 1). A comparison of these curves show that at  $y > 0.05$  the two profiles differ only slightly, while at a distance  $k$  from the step they almost merge. It is interesting to note that for the roughness distribution considered the velocity profile in the plane  $x = 0$  calculated by both methods coincides with the Hartmann profile if  $1 - \bar{\Delta}$  is taken as the half-width of the flow between surfaces.

4. **Resistance coefficient.** As distinct from smooth tubes, in which the resistance is determined only by

friction, in rough tubes the over-all resistance is composed of a friction component and a component depending on the shape of the surface irregularities. Therefore the resistance can be calculated as follows:

$$F = \mu \int \frac{d\bar{u}}{d\bar{y}} d\bar{x} + \int \bar{p} d\bar{y}, \quad (17)$$

where  $\bar{p} = \rho u_m^2 p$ ;  $\bar{u} = u_m u$ ;  $\bar{x} = R x$ ;  $\bar{y} = R y$ . The first term in expression (17) corresponds to the friction resistance and the integral is taken along the lines AB, CD, EF, while the second term is the shape component and the integral is taken along the lines BC, DE. Hence for the resistance coefficient  $\lambda_r$ , the ratio of the resistance F per unit length of flow to the dynamic pressure, we obtain

$$\lambda_r = \frac{1}{a} \left[ \frac{2}{Re} \int (-\xi) dx + 2 \int p dy \right]. \quad (18)$$

Figure 5 presents values of the resistance coefficient for a rough tube divided by the resistance coefficient  $\lambda_s$  for flow between parallel surfaces in the absence of roughness. It is clear from Fig. 5 that with increase in the Hartmann number M the relative resistance coefficient  $\lambda_r/\lambda_s$  increases considerably. The calculated points were obtained at different values of Re (50, 200, 600); however, they all lie on a single curve.

The increase in relative resistance coefficient with increase in Hartmann number is confirmed by experiment when the irregularities of the surface are sufficiently thickly distributed. The experiments were performed on tubes with uniform granular (sandy) roughness on the apparatus described in [9]. The dimensions of the rectangular tube section were  $50 \times 9$  (mm), the relative roughness 0.105. The distance between sand grains was about half the height of the surface irregularities. The experimental values of

$\lambda_r$  obtained in the range of Re numbers from 300 to 600 divided by the resistance coefficient  $\lambda_s$  for a smooth rectangular tube measuring  $50 \times 10$  (mm) are plotted in Fig. 5. The experimental and theoretical curves are qualitatively the same, although quantitative agreement could not be expected.

The physical reasons for the increase in relative resistance coefficient  $\lambda_r/\lambda_s$  with increase in the magnetic field become clear upon examining Figs. 2 and 3. The first of these figures indicates an increase in the effective height of the surface irregularities with increase in Stewart number, the second an increase in the pressure difference between the front and rear faces of the irregularity.

#### REFERENCES

1. J. Nikuradse, VDI, Forschungsheft, 361, 1933.
2. R. K. Dukure, Magnitnaya gidrodinamika [Magnetohydrodynamics], 2, 109, 1966.
3. K. Hidaka, Mem. of Imperial Marine Obs., Kobe, 7, 21, 1939.
4. M. Kawaguti, Journ. Phys. Soc. Japan, 16, 12, 2307, 1961.
5. L. M. Simuni, PMTF [Journal of Applied Mechanics and Technical Physics] 6, 106, 1965.
6. I. S. Berezin and I. N. Zhidkov, Computation Methods [in Russian], GIFML, 1962.
7. N. P. Zhidkov, A. A. Korneichuk, A. L. Krylov and S. B. Mostinskaya, in: Computer Methods and Programming [in Russian], Izd. MGU, 152, 1962.
8. Kh. E. Kalis, A. B. Tsinober, A. G. Shtern, and E. V. Shcherbinin, Magnitnaya gidrodinamika [Magnetohydrodynamics], 1, 18, 1965.
9. R. K. Dukure, Magnitnaya gidrodinamika [Magnetohydrodynamics], 1, 29, 1965.

15 February 1967